Crimson Publishers
Wings to the Research

Research Article

Enhancing Chemotherapeutic Efficacy in Neuroblastoma and Glioblastoma with Extracts of *Piper longum* and *Camellia sinensis*

Darcy Wear[1,2], Karolina Konior[1], Michael Okoko[1], Caleb Vegh[1], Ibrahim Alsalkhadi[1], Victoria Iannetta[1], and Siyaram Pandey[1]*

[1]Department of Chemistry and Biochemistry, University of Windsor, Windsor, Canada

[2]Department of Pharmacology and Toxicology, University of Toronto, Toronto, Canada

ISSN: 2637-7802

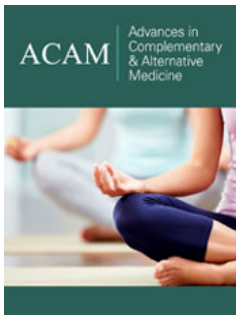

***Corresponding author:** Department of Chemistry and Biochemistry, University of Windsor, Windsor, Canada

Submission: July 15, 2026
Published: July 28, 2026

Volume 9 - Issue 3

How to cite this article: Darcy Wear, Karolina Konior, Michael Okoko, Caleb Vegh, Ibrahim Alsalkhadi, Victoria Iannetta, and Siyaram Pandey*. Enhancing Chemotherapeutic Efficacy in Neuroblastoma and Glioblastoma with Extracts of *Piper longum* and *Camellia sinensis*. Adv Complement Alt Med. 9(3). ACAM. 000711. 2026.
DOI: 10.31031/ACAM.2026.09.000711

Abstract

Glioblastoma is an aggressive brain tumour with 5-year survival rates of just 6.8%, while neuroblastoma accounts for 15% of pediatric cancer deaths. Standard treatment options have limited effectiveness and lack specificity, resulting in severe adverse effects and diminished quality of life. Alternatively, natural health products, used in traditional medicines and safe for long-term consumption, may possess anti-cancer activity. Specifically, whole extracts of *Piper longum* (LPE) and *Camellia sinensis* (STE) have demonstrated selective antineoplastic activity in cancer. This study investigates their potential as novel therapeutics for glioblastoma and neuroblastoma which may be used alongside standard treatments. We posit these extracts exhibit both selective standalone anti-cancer activity and interact positively with chemotherapeutics, targeting the bulk tumour and cancer stem cells. Indeed, *in-vitro* experiments demonstrated LPE- and STE-induced apoptosis in glioblastoma and neuroblastoma, mediated by oxidative stress and mitochondrial destabilization respectively. Importantly, our extracts did not impede chemotherapeutic efficacy in combination treatments. These findings indicate the potential of STE and LPE as safe and effective adjuvant therapeutics in both glioblastoma and neuroblastoma. Their use may enable reduced chemotherapy dosages, minimizing adverse effects and providing a promising avenue for preventing cancer relapse. Further investigation, including clinical studies, is warranted to validate these therapeutic benefits.

Keywords: Apoptosis; Cancer; Glioblastoma; Natural health products; Neuroblastoma; Oxidative stress

Abbreviations: AV: Annexin V; BBB: Blood-Brain-Barrier; CSC: Cancer Stem Cell; DCF: 2,7-Dichlorofluorescein; DMSO: Dimethyl Sulfoxide; GBM: Glioblastoma; GSC: Glial Cancer Stem Cell; JNK: Jun N-terminal Kinase; LPE: Long Pepper Extract; MMP: Mitochondrial Membrane Potential; NAC: N-Acetyl Cysteine; NB: Neuroblastoma; NHP: Natural Health Product; PBS: Phosphate-Buffered Saline; PI: Propidium Iodide; ROS: Reactive Oxygen Species; STE: Synthite Tea Extract; TBST: Tris-Buffered Saline, 0.1% Tween 20 Detergent; TMRM: Tetramethylrhodamine, Methyl ester; TMZ: Temozolomide; WST: Water-Soluble Tetrazolium Salt

Introduction

Neuroblastoma (NB) is responsible for 15% of pediatric cancer deaths as it remains a highly prevalent infancy cancer [1]. Despite recent therapeutic advancements in patients with high-risk NB, 5-year survival rates remain approximately 50% [2]. Furthermore, standard therapeutic options for NB have significant drawbacks including many adverse effects. One clinical study reported grade 3 or 4 hematologic effects in all patients as well as serious

infection or sepsis in 53% of patients receiving continuous cisplatin treatment, a standard chemotherapy used in the treatment of NB [3]. Thus, significant advancements in our current treatment strategies are required to improve prognosis, ameliorate the negative impacts of current therapies, and enhance long-term safety. Another cancer of the neural tissue, Glioblastoma (GBM), is the most prevalent primary brain tumour, accounting for 48.6% of malignant central nervous system tumours and 14.5% of all nervous system tumours [4]. Since GBM typically affects older individuals, with a median diagnosis of 64 years, prevalence rates are expected to increase with the growing and aging population [5,6].

Despite advancements in diagnostic imaging, the prognosis associated with GBM remains extremely poor with a 5-year survival rates around 5% [5,7]. As with most cancers, maximal surgical resection is the primary treatment option for all GBM patients, followed by combinations of chemotherapy and radiotherapy [8]. Radiation therapies are effective at inducing apoptosis in GBM tumours through significant DNA damage. However, the increased efficiency of DNA double-stranded break repair machinery in many tumours promotes the development of radiotherapy resistance [9]. Temozolomide (TMZ) is the standard chemotherapy utilized in GBM treatment, functioning as a DNA alkylating agent to induce apoptosis [10]. Similar to radiotherapy, TMZ is a genotoxic therapy and, therefore, poses significant risk due to the severity of DNA damage incurred on normal healthy cells [11]. Treatment resistance and the negative side-effects of these drugs support the notion that improved therapeutic options are necessary. A primary reason for poor survival rates in many cancers, including GBM, is the presence of Cancer Stem Cells (CSCs), a small subpopulation of carcinogenic cells with self-renewal capabilities [12].

Current anti-cancer treatments that do not explicitly target CSCs may shrink tumours without preventing tumour regrowth, leading to relapse. Specifically, treatment options in GBM are limited by the presence of self-renewing, Glial Cancer Stem Cells (GSCs) [12,13]. GSCs are responsible for several tumorigenic features including angiogenesis, apoptotic evasion, genomic instability, and uncontrolled cellular proliferation, promoting overall disease progression [14,15]. CSCs are often distinguished from other tumor cells through single and combinatory cell surface biomarkers. Commonly used as a GSC marker, CD44 isn't strictly found in CSCs, but elevated expression levels in GBM are associated with enhanced tumour proliferation and invasiveness [16]. Adjuvant therapeutics alongside chemotherapy that can target these cells could reduce tumorigenesis associated with CSCs. Natural Health Products (NHPs) provide promise as a potentially effective and tolerable option for long-term cancer treatment. With many NHPs used in traditional Indian and Chinese medicines, and various chemotherapies including vinblastine and paclitaxel derived from plants, it is possible that other plant-derived extracts may possess anti-cancer activity with limited adverse effects [17-19].

Specifically, our lab has demonstrated the selective anti-cancer capabilities of NHPs including long pepper, white/green tea, dandelion root, lemongrass, and hibiscus in a variety of cancers [20-26]. Despite previous work demonstrating the anti-cancer activity of *Piper longum* (long pepper) on colon, ovarian, pancreatic, leukemia, and melanoma cancers, and *Camellia sinensis* (tea) on lymphoma and breast cancer, their specific effects both alone and combined with standard chemotherapeutics has not been analyzed in models of NB or GBM. Furthermore, their relapse-prevention potential by targeting CSCs has not been investigated. Long Pepper Extract (LPE) contains bioactive compounds including piperine and piperlongumine, which possess anti-cancer activity through the elevation of oxidative stress [27,28]. Green tea from the *Camellia sinensis* plant is known to contain polyphenols, including several types of catechins like epigallocatechin 3-gallate [29,30]. Contrary to LPE, this compound possesses strong antioxidative properties, but displays anti-cancer activity and can sensitize CSCs to chemotherapy [29-33].

Despite this knowledge, the effect of these whole extracts on cancers of the neural tissue, including NB and GBM, remains largely unknown. This project sought to investigate the anti-cancer capabilities of LPE and Synthite Tea Extract (STE), in NB and GBM models, including CD44-positive (CD44+) cells. Importantly, we investigated their interactions with standard chemotherapeutics to ensure their safety for clinical trials as an adjuvant therapy. We demonstrate the significant anti-cancer capabilities of ethanolic LPE and aqueous STE, inducing apoptosis in both NB and GBM models in a dose-dependent manner. Critically, we have shown that, LPE, and to a greater extent STE, interact positively with standard chemotherapeutics cisplatin and TMZ. Due to their safe long-term usage, we have also showed the prospect of both LPE and STE in the prevention of cancer relapse, by minimizing the CD44+ GSC-like population in GBM cancer models. As a result, both LPE and STE possess great therapeutic potential to be utilized as alternate therapeutics to current treatments or alongside them as an adjuvant in both GBM and NB patients.

Results

LPE and STE possess anti-cancer activity against neuroblastoma and glioblastoma

To determine whether our whole extract of *Piper longum* (LPE) possessed significant anti-cancer activity, we performed AV and PI staining with image-based cytometry to measure early-stage apoptosis and late-stage apoptosis/necrosis respectively in SH-SY5Y neuroblastoma and U-87 Mg glioblastoma cells (Figure 1a). LPE induced apoptosis in both cell lines at the 24-hour timepoint ($p<0.0001$ at 0.05mg/mL) following treatment compared to the Dimethyl Sulfoxide (DMSO) control. Similarly, we demonstrated the potent, dose-dependent anti-cancer activity of STE in SH-SY5Y cells after 24 hours ($p=0.0002$ at 0.15mg/mL-Figure 1b). In GBM however, STE showed time-dependence, only inducing significant apoptosis following 48-hour treatments ($p=0.0063$ at 0.1mg/mL-Figure 1c). As a proof of concept in a more architecturally accurate context, U-87 Mg cells were seeded on 8-chamber slides coated with Matrigel basement membrane, allowing for intracellular scaffolding that guided three-dimensional structures. Spheroid

formation was monitored for 96 hours, followed by treatment with LPE or STE and subsequent observation for 96 hours. We observed morphological signs of apoptosis and spheroid disruption through brightfield micrographs (Figure 1d).

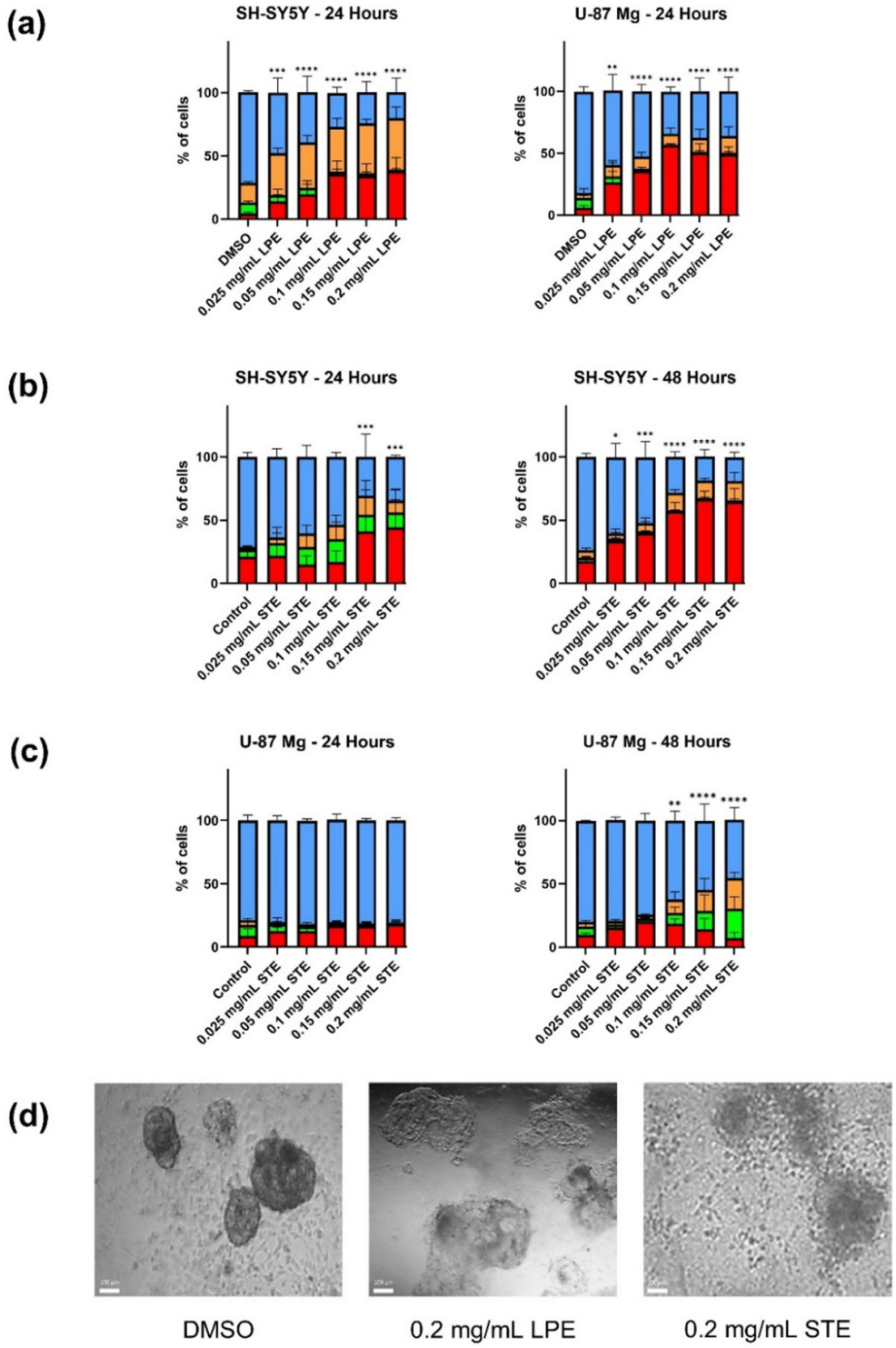

Figure 1: Dose and time-dependent apoptotic induction in NB and GBM. (a) LPE induced apoptosis in NB and GBM after a 24-hour treatment. (b) STE induced apoptosis in SH-SY5Y cells and (c) U-87Mg cells in a time-dependent manner. Cells were treated with LPE or STE for 24- or 48-hours using AV and PI staining with image-based cytometry to quantify percentages of apoptotic cells compared to the DMSO control. Blue bars indicate viable cells, green bars indicate AV staining, red bars indicate PI staining, and orange bars indicate both AV and PI. Values are expressed as mean±SD from 3 independent experiments. (d) LPE and STE disrupt 3D GBM spheroids after 96-hour treatment. 3D spheroids were imaged with brightfield microscopy to observe morphological changes after 96-hour treatment. Micrographs were taken at 200x magnification.

LPE and STE target GSCs and reduce metastatic behaviour in NB

Immunofluorescent analysis was conducted to assess changes in the glial cancer stem-like cell population following treatment with LPE and STE. CD44 expression, a commonly used marker for GBM stem-like cells, was used to visualize and quantify this population in U-87 Mg cultures. After 48hours of treatment, both LPE and STE resulted in a visibly reduced proportion of CD44+ cells relative to the DMSO control, with the effect being more pronounced in STE-treated samples (Figure 2). Treatment with TMZ, by contrast, had limited effects on the CD44+ population. These qualitative findings suggest that both extracts-particularly STE-may reduce the stem-like cancer cell subpopulation, which could contribute to their overall therapeutic potential against treatment-resistant GBM. To examine whether these extracts limit cancer cell motility, a wound healing assay was conducted.

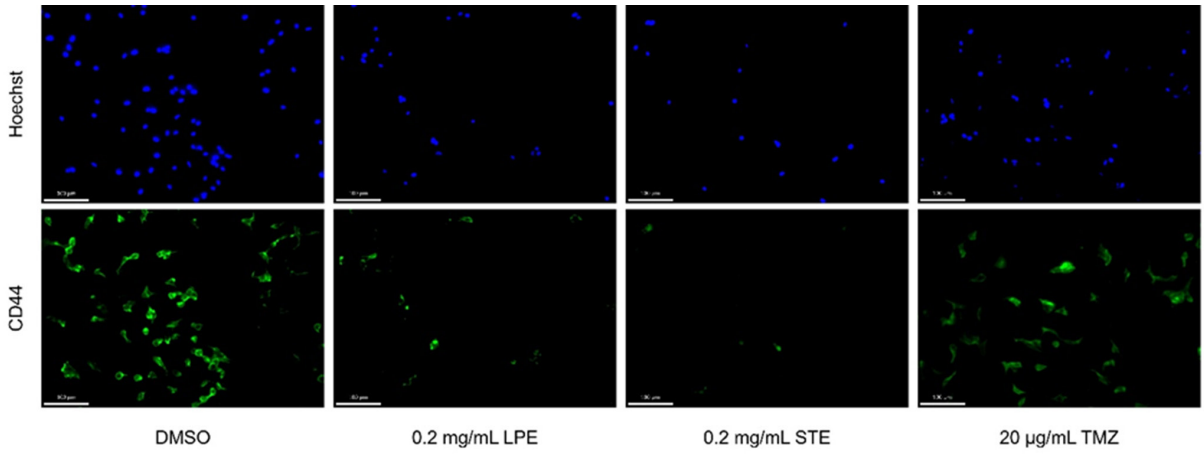

Figure 2: STE and LPE reduce the proportion of CD44+ U-87 Mg cells. Cells were probed for CD44 (green) following 48-hour treatment with DMSO, LPE, STE, or TMZ and imaged with fluorescent microscopy. We observed a reduced proportion of CD44+ positive in cells treated with STE and to a lesser extent, LPE. TMZ did not appear to influence the proportion of CD44+ cells relative to DMSO control. Images are representative of a minimum of 6 randomly selected independent fields. Nuclei were counterstained with 10µM Hoechst. Micrographs were taken at 200x magnification.

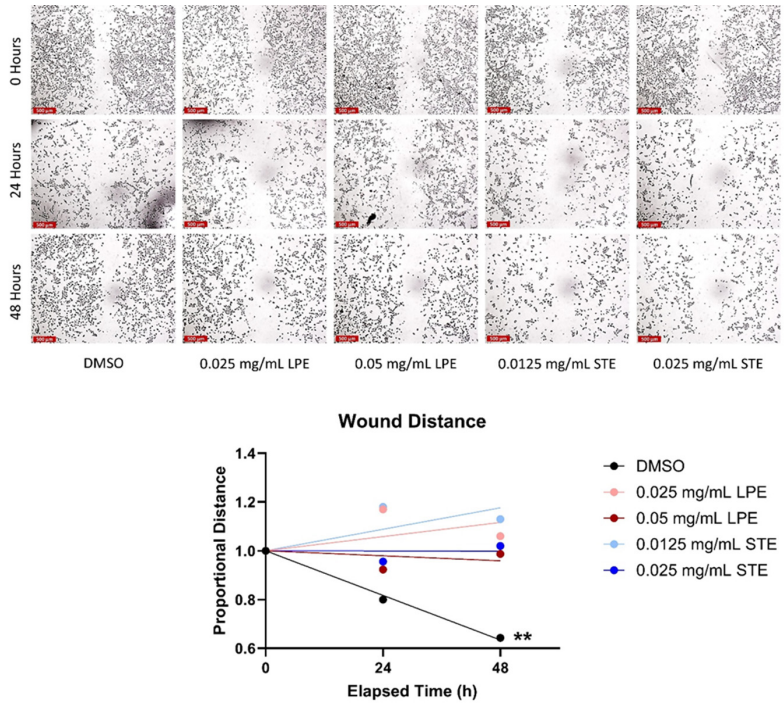

Figure 3: LPE and STE limit SH-SY5Y cell motility. Cells were mechanically scraped in the centre of each well and imaged with phase contrast microscopy at 0-, 24-, and 48-hour timepoints. The gap between cells on either side (wound size) was measured at each time point. Treatment of cells with LPE or STE inhibited gap distance closure and cell migration. Simple linear regression was conducted on each group with only the DMSO control have a slope significantly non-zero (p=0.001). Micrographs were taken at 40x.

SH-SY5Y neuroblastoma cells were pre-treated for 18-hours with thymidine to halt cell proliferation and subsequently scratched with a sterile P200 pipet tip. Cells were treated with sub-lethal doses of LPE or STE and imaged through phase contrast microscopy at the 0-, 24-, and 48-hour timepoints. The gap-width of the wound was measured at each time point and compared to an untreated control. Results are expressed as proportional distance to account for differences in initial gap width between samples with each initial distance set to a value of 1. Using a linear regression model, we observed a significant reduction in the gap width in the control group (p=0.001) which was prevented by the addition of LPE or STE (Figure 3).

LPE and STE enhance the anti-cancer activity of standard chemotherapeutics cisplatin and TMZ

After demonstrating the apoptosis-inducing ability of both LPE and STE alone, we sought to examine their interactions with standard chemotherapeutics cisplatin and TMZ. Image-based cytometry and epifluorescence microscopy coupled with AV and PI staining were utilized in SH-SY5Y cells (Figure 4) to determine the interactions between LPE, STE, and cisplatin. No statistical differences were observed between cisplatin treatment alone and cisplatin with LPE at any tested dose (Figure 4a). Although, under fluorescent microscopy, it appeared that there may be some beneficial effect to the addition of LPE (Figure 4b). Alternatively, STE significantly increased apoptotic levels when combined with cisplatin at doses of 1μM (p=0.0493) or 5μM cisplatin (p=0.0002). In U-87 Mg GBM cells, a high-throughput WST-1 assay was used alongside AV/PI fluorescent microscopy to examine interactions between these extracts and the commonly used chemotherapy TMZ (Figure 5). At TMZ doses of 4μg/mL or 25μg/mL, we observed a reduction in cell viability with the addition of 0.1mg/mL LPE (p=0.0209 at 4μg/mL; p=0.0265 at 25μg/mL). Once again, STE was able to significantly reduce cell viability at all tested doses of TMZ (p<0.0001 at 4μg/mL TMZ, p=0.0005 at 25μg/mL TMZ, p=0.0229 at 50μg/mL and p=0.0229 at 75μg/mL TMZ). Interestingly, the combination of LPE and STE appears more effective at diminishing cell viability than any combination containing TMZ.

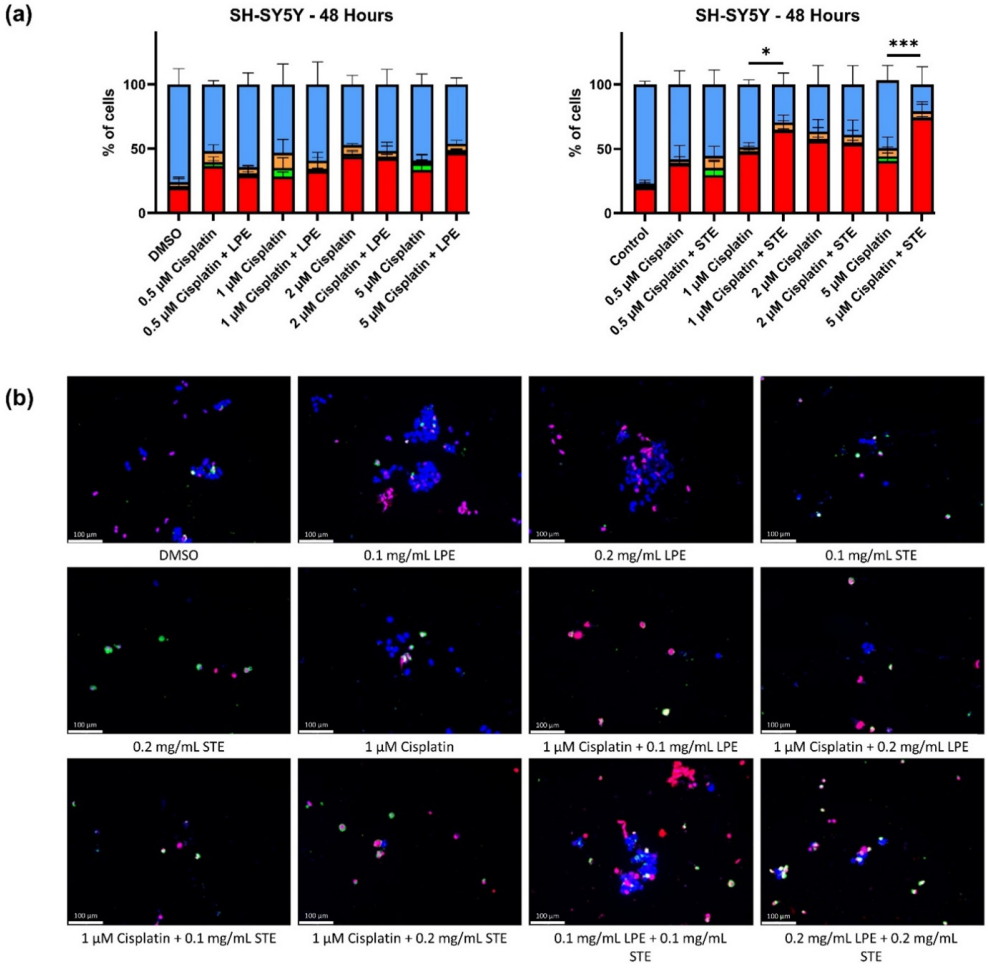

Figure 4: STE enhances the anti-cancer activity of cisplatin while LPE has no significant effect in SH-SY5Y neuroblastoma cells. AV (green) and PI (red) staining on SH-SY5Y followed by (a) quantifiable image-based cytometry or (b) epifluorescence microscopy was performed to analyze the combinatorial effect of LPE and STE with the standard chemotherapeutic cisplatin. 0.1mg/mL LPE had no significant impact on cisplatin-induced cell death at any dose while 0.1mg/mL STE enhanced apoptotic levels at doses of 1μM and 5μM cisplatin. Nuclei were counterstained with 10μM Hoechst. Values are expressed as mean±SD from 3 independent experiments. Micrographs were taken at 200x magnification.

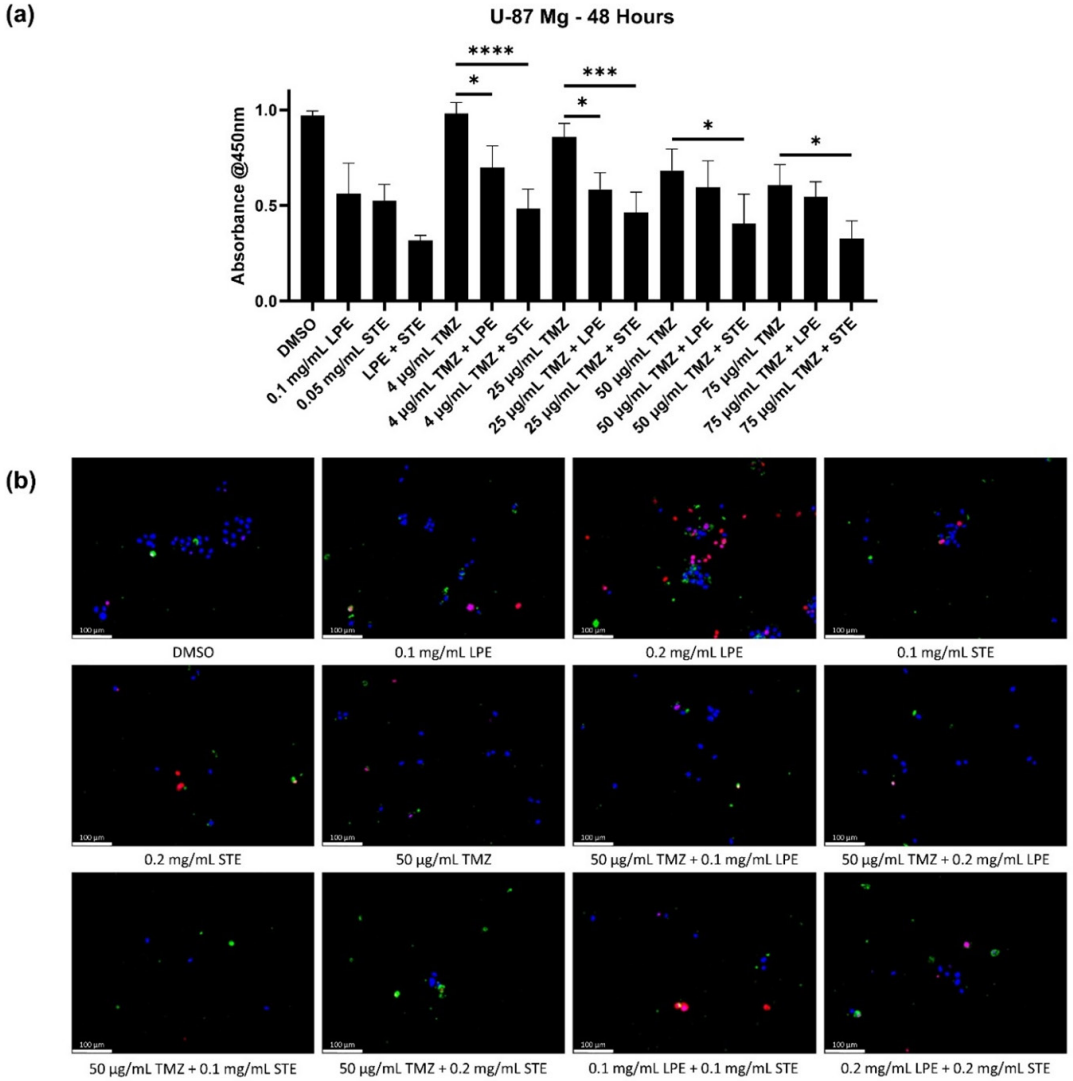

Figure 5: LPE and STE reduce the number of viable U-87 Mg cells in combination with the standard chemotherapy TMZ. (a) WST-1 assay and (b) AV (green) and PI (red) staining on U-87 Mg followed by epifluorescence microscopy was used to examine the combinatorial effect of LPE and STE with the standard chemotherapeutic TMZ. LPE reduced cell viability alongside TMZ at lower doses of 4µg/mL and 25µg/mL compared to TMZ alone while STE enhanced cell death at all doses of TMZ. Nuclei were counterstained with 10µM Hoechst. Values are expressed as mean±SD from 3 independent experiments. Micrographs were taken at 200x magnification.

LPE and STE target multiple mechanisms in cancer cells

U-87 Mg and SH-SY5Y cells were subjected to TMRM staining to analyze their MMP following treatment with LPE or STE. 24-hour treatment of the U-87 Mg cells followed by image-based cytometry showed diminished MMP in cells treated with either extract ($p=0.0034$ for LPE, $p=0.0016$ for STE-Figure 6a). A prolonged 48-hour treatment of the SH-SY5Y cells imaged with epifluorescence microscopy showed slightly reduced TMRM staining in LPE-treated cells and drastically decreased fluorescence in cells treated with STE (Figure 6b). Next, 2,7-Dichlorofluorescein (DCF) fluorescent staining followed by image-based cytometry or epifluorescence microscopy allowed for the visualization and quantification of ROS following 3-hour (Figure 7a) and 24-hour (Figure 7b) treatments with LPE and STE. We observed a significant induction of ROS in cells treated with LPE alone compared to DMSO control ($p=0.0003$ in SH-SY5Y; $p<0.0001$ in U-87 Mg) or with LPE-chemotherapy combinations compared to chemotherapy alone ($p<0.0001$ for SH-SY5Y; $p=0.0031$ for U-87 Mg). STE treatment alone had no significant effect on oxidative stress but did reduce the ROS induction caused by TMZ treatment alone ($p=0.0036$). To determine whether LPE-induced oxidative stress was critical to its anti-cancer activity, we treated SH-SY5Y and U-87 Mg cells with LPE alone and LPE with N-Acetyl Cysteine (NAC), a known antioxidant. These cells were then subjected to AV and PI staining followed by epifluorescence microscopy to examine cell death (Figure 7c-d). Indeed, there was a diminished apoptotic response in the presence of NAC implicating the dependence on ROS for LPE-induced apoptosis.

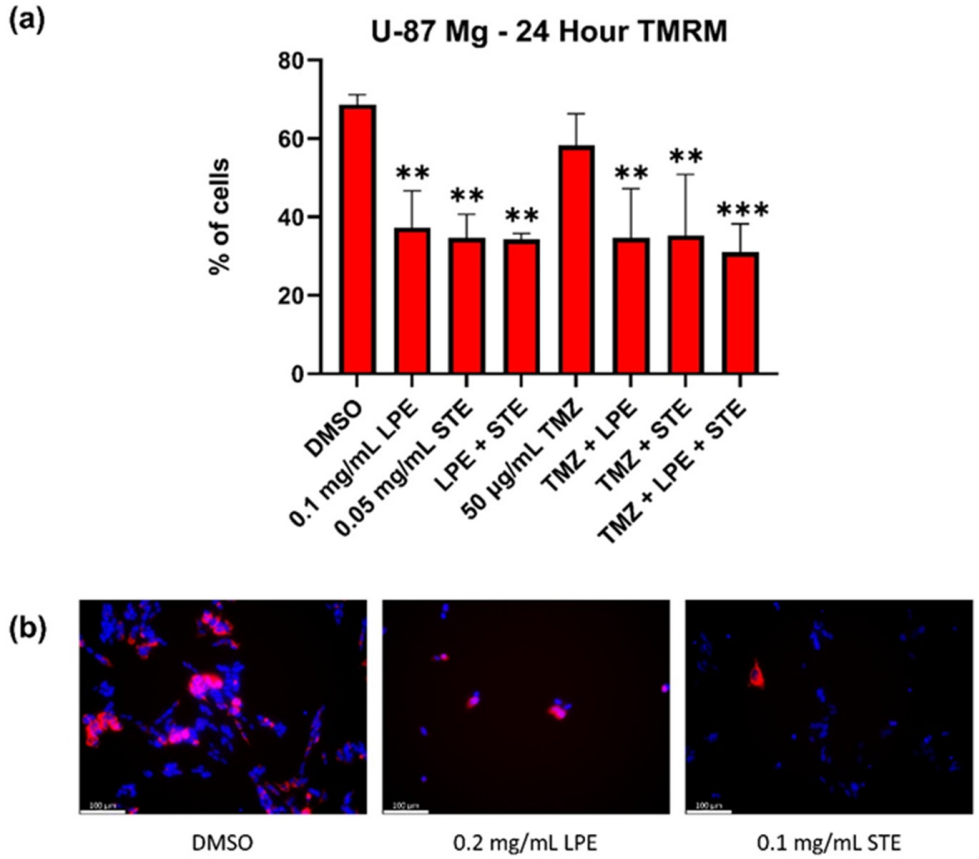

Figure 6: LPE and STE reduce mitochondrial stability in both U-87 Mg and SH-SY5Y cells. TMRM (red) live cell mitochondrial staining was performed on (a) U-87 Mg after 24-hour treatments and analyzed via flow cytometry and (b) SH-SY5Y after 48-hour treatments and visualized with epifluorescence microscopy. LPE and STE diminished the MMP in NB and GBM cell lines alone and in combination with TMZ. Nuclei were counterstained with 10µM Hoechst. Values are expressed as mean ±SD from 3 independent experiments. Micrographs were taken at 200x magnification.

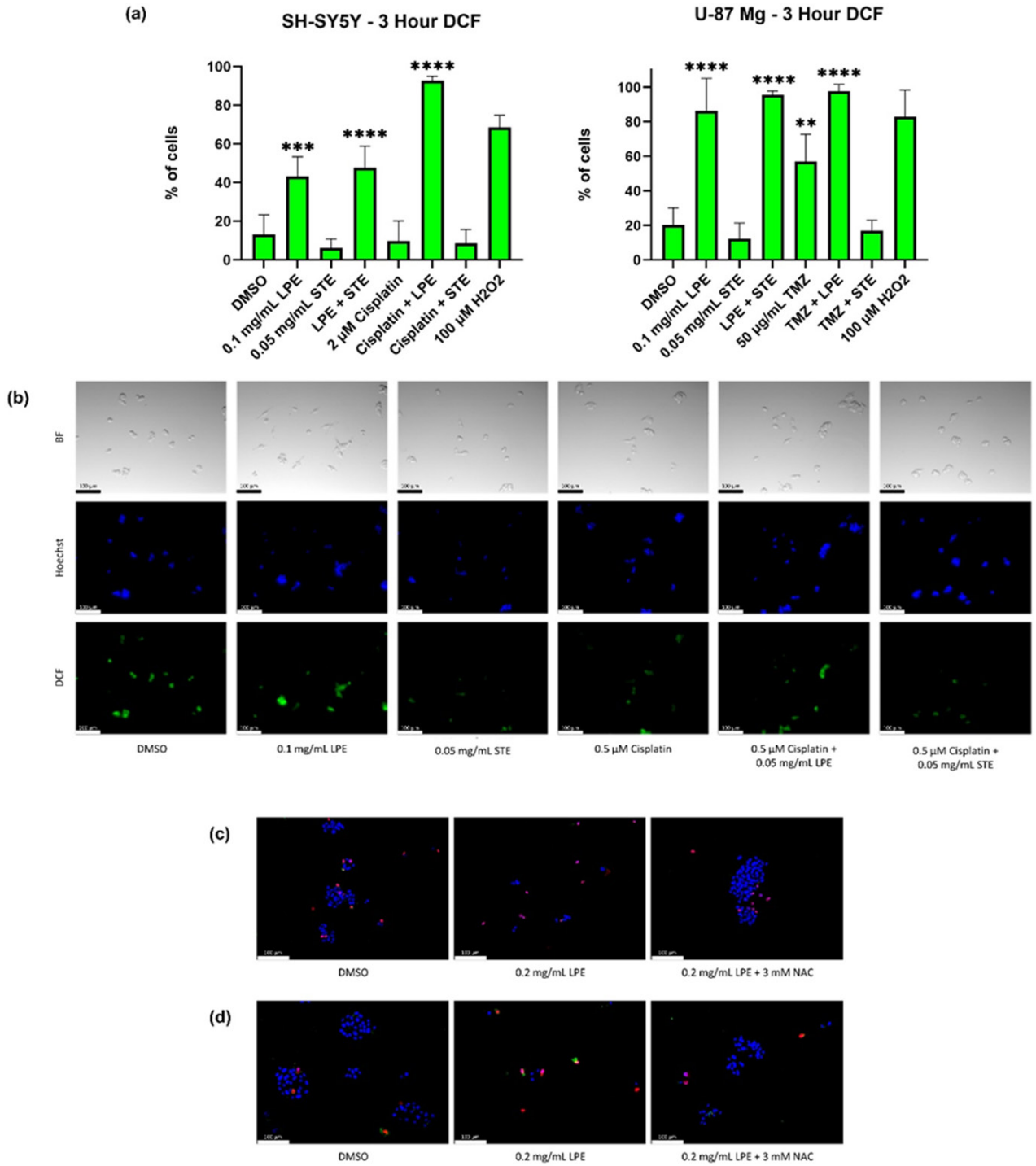

Figure 7: LPE-induced apoptosis is dependent on the generation of oxidative stress in SH-SY5Y and U-87 Mg cells. H2DCFDA (green) staining was performed on (a) SH-SY5Y and U-87 Mg cells following 3-hour treatments with LPE and STE and quantified with image-based cytometry, and on (b) SH-SY5Y after 24-hours followed by epifluorescence microscopy. AV (green) and PI (red) staining followed by epifluorescence microscopy was done on (c) SH-SY5Y and (d) U-87 Mg cells treated with LPE and the antioxidant NAC. LPE significantly elevated oxidative stress in NB and GBM cells when used alone or in combination with STE, cisplatin, or TMZ. LPE-induced apoptosis was reduced when combined with the antioxidant NAC. STE reduced oxidative stress levels when combined with TMZ but had no significant impact on its own. Nuclei were counterstained with 10µM Hoechst. Values are expressed as mean±SD from 3 independent experiments. Micrographs were taken at 200x magnification.

LPE-induced apoptosis specific to cancerous cells

To examine the previously untested specificity of our LPE, we treated normal colon epithelial cells (NCM-460) for 48hours and performed AV/PI staining with image-based cytometry (Figure 8a). LPE treatment resulted in no significant apoptotic induction at doses up to and including 0.5mg/mL indicating a high specificity

towards cancer cells. To mechanistically assess LPE's specificity, we examined its influence on ROS levels in NCM-460 through DCF fluorescent staining and image-based cytometry (Figure 8b). Indeed, no significant induction of ROS was seen in these normal cells as it was in both SH-SY5Y and U-87 Mg cell lines. Previously, our lab showed no significant apoptotic induction with STE treatment in NCM-460 at doses up to and including 0.25mg/mL [26]. To confirm these results *in-vivo*, we gave male Foxn1nu/Foxn1nu immunocompromised mice, aged 5 weeks, 0.4mg/mL STE (approximately 95mg/kg/day) supplemented in their drinking water ad libitum or 50mg/kg/injection LPE through intraperitoneal injection 3x/week (n=4) for one month. Liver, heart, and kidney tissues were extracted post-mortem and sent to the University of Guelph Animal Health Laboratory for histopathological analysis. The pathological report can be found in the supplemental data with groups C1 (control), T5 (LPE), and T6 (STE) relevant to this project. ¼ sections from LPE-injected animals showed mild mononuclear cell clustering in the liver while no effects on heart of kidney sections were observed. Liver sections of STE-treated animals showed no additional pathology compared to control while kidney (1/6) and heart (2/6) displayed minimal to mild histological lesions (supplemental pathology report). We also found no changes in mouse weight over a month period compared to the untreated control (p=0.9397) (Supplemental Figure 1).

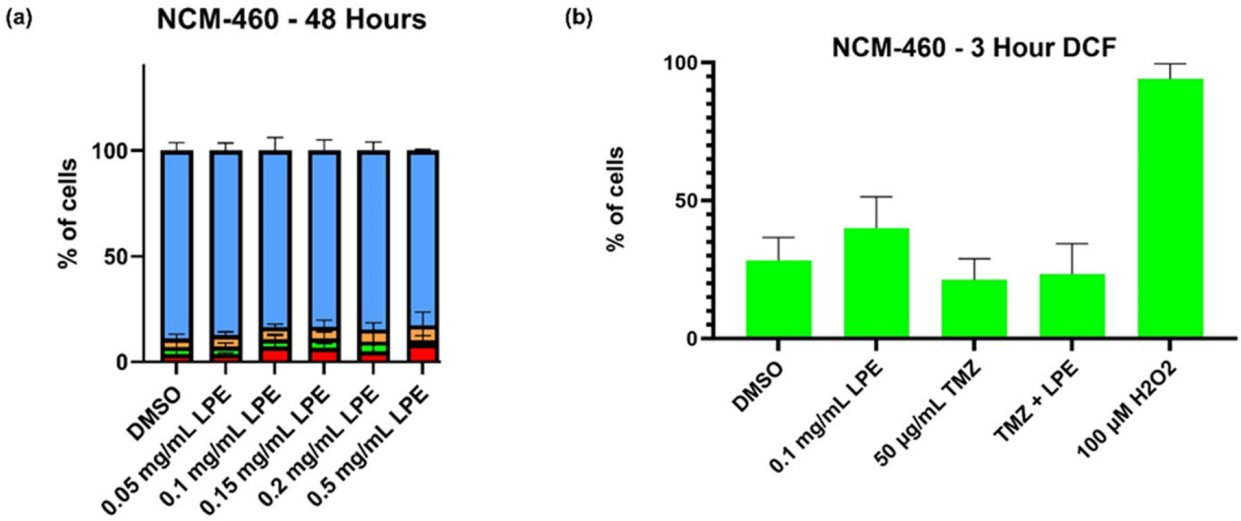

Figure 8: LPE is non-toxic to normal colon epithelial cells after 48-hour treatment. (a) AV and PI staining were used alongside image-based cytometry to examine cell death in NCM-460 cells after 48-hour treatment with LPE. LPE did not induce apoptosis at doses up to and including 0.5mg/mL in these non-cancerous cells. (b) Cells were stained with H2DCFDA and examined for ROS levels via image-based cytometry after 3-hour treatment with LPE. No significant oxidative stress occurred following LPE. Values are expressed as mean±SD from 3 independent experiments.

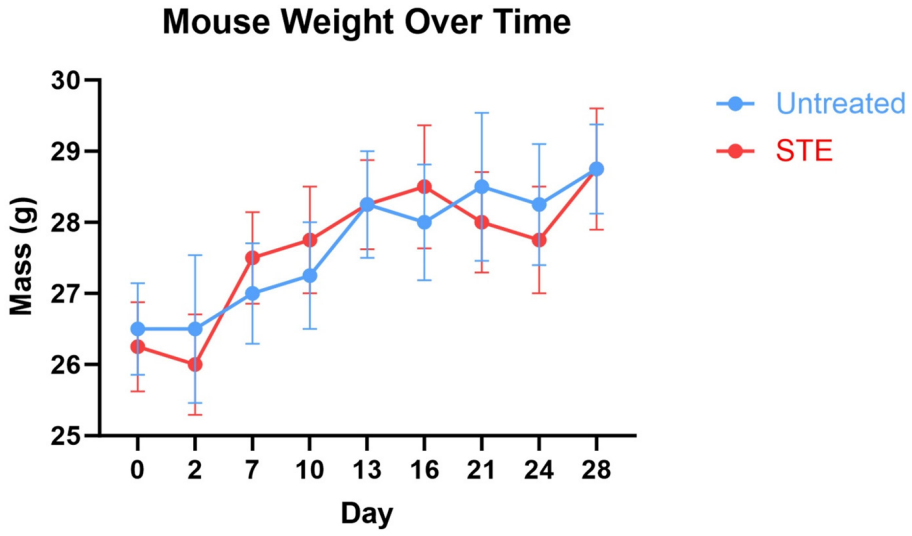

Supplemental Figure 1: STE supplementation does not affect mouse weight gain over a month treatment period. Mice were given 0.4mg/mL STE in their drinking water for 1 month and weight gain was monitored. No difference was observed between treatment groups (p=0.9397, 2-way ANOVA). n=4/group. Values are expressed as mean±SD.

Discussion

We have examined two novel therapeutics in LPE and STE for the treatment of both glioblastoma and neuroblastoma. Using U-87 Mg and SH-SY5Y cell lines, we demonstrated the anti-cancer capabilities of these extracts in-vitro where they induced apoptotic cell death, including diminishing CD44+ cell populations, and limited cancer cell motility. LPE treatment resulted in ROS production and mitochondrial destabilization with overall apoptosis onset. STE diminished MMP and significantly reduced cell viability in both GBM and NB. In combination with standard chemotherapeutics, STE exhibited positive interactions while LPE had no significant interaction with cisplatin, but enhanced cell death in combination with TMZ. In support of prior data, these extracts had minimal histological impact *in-vivo* highlighting their selectivity and safety for long-term consumption. Overall, these NHPs are capable of inducing apoptosis in GBM and NB through multiple mechanisms both alone and combined with standard chemotherapeutics with limited toxic effects.

To begin, we determined whether the Piper longum extract possessed apoptosis-inducing capabilities in cellular models of GBM and NB. Active components of Long Pepper, including piperine and piperlongumine, are known to possess anti-cancer effects [28,34-41]. In particular, extensive work with piperlongumine has highlighted its capability to trigger oxidative stress selectively in cancer cells [41]. As a result, we hypothesized that whole extracts of Long Pepper may possess multiple compounds acting synergistically with one another to enhance the anti-cancer effect. Indeed, LPE induced dose-dependent apoptosis in both SH-SY5Y and U-87 Mg cell lines after just a 24-hours treatment (Figure 1a). Similarly, previous research has shown that catechins found in Camellia sinensis possess anti-cancer activity in both prostate and breast cancer [32,33]. With STE treatment, we observed dose- and time-dependent cell death in both NB and GBM cell models (Figure 1b-c). Compared to 2D monolayers, 3D tumor spheroids more accurately reflect tumors, developing natural gradients of oxygen and nutrients that create zones of proliferation, quiescence, and necrosis [42,43].

As a proof of concept, we sought to validate our 2D findings in a more physiologically relevant context. We cultured U-87 Mg glioblastoma cells in Matrigel-coated chamber slides to induce 3D spheroid formation. Following a 96-hour treatment with LPE or STE, we observed morphological signs of apoptosis and varying degrees of spheroid disruption, with LPE inducing partial disintegration and STE leading to extensive fragmentation (Figure 1d). These observations support their cytotoxic effects in a more physiologically relevant context. While the targeting of primary tumors is essential, other factors including tumor heterogeneity, treatment resistance, and metastasis are crucial for patient prognosis. GBM stem-like cells have garnered significant attention due to their proposed role in tumor recurrence and heterogeneity [44]. Therapeutic resistance through quiescence, DNA repair mechanisms, and drug efflux promote survival and drive tumor relapse [45]. CD44, a cell surface glycoprotein associated with stemness and invasiveness, is variably expressed across glioblastoma models. In our study, we examined the sensitivity of this CD44+ subpopulation of U-87 Mg cells to LPE and STE treatment.

Following treatment, we observed a reduction in the proportion of CD44+ cells, particularly in response to STE (Figure 2), suggesting these extracts may diminish stem-cell-like GBM and be crucial to overcoming chemoresistance. Future research should explore whether combinations with chemotherapy limit chemoresistance, reducing tumor relapse and improving patient outcomes. Although extracranial metastasis is a rare occurrence in GBM patients [46], it commonly spreads through the direct invasion of adjacent brain tissues [47]. Conversely, NB frequently metastasizes from the primary tumour site to bone marrow, lymph nodes, the liver, intracranial sites, lungs, and skin [48]. Therefore, we examined the motility of SH-SY5Y neuroblastoma cells treated with low doses of LPE or STE, and thymidine to inhibit cell proliferation, with a Wound Healing assay (Figure 3). Importantly, cell migration was inhibited in LPE and STE treated groups, where the intracellular gap began to close in the untreated group. This concurs with previously published data on STE showing reduced cell motility in MDA-MB-231 breast cancer cells [26].

Despite prior research highlighting the potential therapeutic value of NHPs in cancer treatment, many oncologists are hesitant to allow patients to take these as supplemental treatments due to their unknown interactions with standard chemotherapies. Rightly so, there have been NHPs shown to negatively impact the efficacy of drugs including St. John's Wort which induces hepatic CYP3A4 enhancing drug clearance [49]. Conversely, an active compound in milk thistle has demonstrated hepatoprotective effects in cancer patients when utilized alongside chemotherapeutics [50]. As a result, we sought to determine the in-vitro interaction between LPE and STE and the commonly used chemotherapies TMZ and cisplatin. For the first time, we report that LPE does not negatively impact cancer cell death induced by cisplatin (Figure 4) or TMZ (Figure 5). In fact, LPE and TMZ interact positively at lower doses of TMZ diminishing cell viability compared to TMZ alone. Furthermore, STE significantly enhanced the apoptotic effect of this chemotherapeutics in both SH-SY5Y and U-87 Mg cell lines, indicative of positive interactions.

After observing the clear anti-cancer activity of LPE and STE, we aimed to determine their mechanism(s) of action for inducing apoptosis in NB and GBM. Piperlongumine, a major compound in Piper longum, has been shown previously to target cancerous cells through the induction of ROS [41,51]. Due to the elevated metabolic rates of cancer cells, they produce higher levels of ROS and can be targeted through oxidative stress [52]. In particular, hypoxia contributes to NB progression by maintaining immature, stem-like tumour cells [53], implicating their potential vulnerability to ROS induction. Indeed, we observed a drastic uptick in ROS production in both SH-SY5Y and U-87 Mg cells after treatment with LPE alone or in combination with chemotherapy (Figure 7). Furthermore, we observed that LPE-induced apoptosis was dependent on the generation of ROS as supplementation with a known antioxidant NAC blocked cancer cell death. Alternatively, mitochondrial vulnerabilities often arise due to changes in the MMP as a result

of the Warburg Effect. This states that the cellular metabolism of cancerous cells favours lactic fermentation rather than aerobic respiration resulting in the generation of an acidic cytoplasm [54]. Examining the MMP, LPE was able to diminish it significantly in U-87 Mg cells (Figure 6), likely an outcome of significant oxidative stress [55].

Conversely, EGCG, a polyphenol found in Camellia sinensis, has been shown to target receptor tyrosine kinases to inhibit cell proliferation and disrupt the MMP through the Jun N-Terminal Kinase (JNK) pathway, whereby JNK phosphorylates the pro-apoptotic protein BAX triggering its migration and disruption of the MMP [56-59]. Interestingly, these same catechins are responsible for the known anti-oxidative capabilities of green tea [29,30]. In support of this, we observed STE significantly diminish MMP (Figure 6) while having little effect on ROS when used alone (Figure 7). In combination with LPE, STE did not reduce oxidative stress levels, suggesting that LPE will still induce ROS-dependent apoptosis. Though STE did reduce ROS levels produced by TMZ in U-87 Mg cells, TMZ's main mechanism is that of a DNA alkylating agent causing eventual cell cycle arrest [60]. Furthermore, it has been suggested that antioxidants may enhance chemotherapy effects by blocking the generation of oxidative-stress induced aldehydes which can inhibit death receptors and caspases [61]. As a result, STE enhances rather than preventing GBM cell death following TMZ treatment.

Despite regular green tea consumption worldwide, and its many known health benefits, there have been reports of toxicological effects ranging from acute to chronic associated with tea extracts and EGCG [62]. Conversely, in a human brain microvascular endothelial cell model of Alzheimer's Disease, a green tea extract provided overall brain protection through its antioxidant capabilities [63]. As our lab has previously shown a lack of toxicity in-vitro for STE [26], we wanted to confirm tolerability using an immunocompromised mouse model. Limited toxicity was observed *in-vivo* as ad libitum STE supplementation resulted in mild myocardial necrosis in 2/6 heart tissue sections, minimal epithelial cell hypertrophy in the kidney, and no negative hepatic effects (supplemental pathology report). Furthermore, all mice receiving STE in their drinking water gained weight in a similar fashion to the untreated control mice (Supplemental Figure 1). Therefore, we conclude that STE is relatively safe for consumption with the possibility of mild side-effects.

Though limited toxicological data exists on whole extracts of Piper longum, previous research has examined potential toxicity associated with its main constituents piperlongumine and piperine. Piperlongumine treatment in mice resulted in no change to mouse or organ weight with no irreversible toxicological effects to the liver, spleen, or kidney [64,65]. Crucially, piperlongumine ameliorated 5-flourouracil induced leukocytopenia inciting protective effects as well. Piperine has shown high selectivity to cancer cells in-vitro with no toxicity to human lung fibroblasts or human intestinal cells [66,67]. In concurrence, we showed that LPE did not induce apoptosis in NCM-460 cells with doses up to 20x larger than those lethal to SH-SY5Y or U-87 Mg cells (Figure 8a). Coinciding with this, LPE did not promote ROS formation in these cells (Figure 8b). Certain genes like Sirtuin1 that are critical in aging and survival and senescence could play a role in the glioblastoma and neuroblastoma development, and could be investigated in future [68], Limited *in-vivo* toxicity occurred with histopathological analysis indicating mild centrilobular perivascular clustering of mononuclear cells in 1 out of 4 livers, with no effects on the heart or kidneys following IP LPE injections (Supplemental Method).

Supplemental Methods

Male Foxn1nu/Foxn1nu immunocompromised mice, aged 5 weeks, were obtained from The Jackson Laboratory (Cat. No. 007850, Bar Harbor, ME, USA). The authors adhered to ARRIVE guidelines and all protocols were followed using appropriate guidelines and regulations approved by the University of Windsor Animal Care Committee (AUPP #20-02) in accordance with the Canadian Animal Care Committee in a laboratory setting with 12-hour light/dark cycles. Mice were placed into 1 of 3 groups: Untreated Control (n=4), STE drinking water (n=4), or LPE IP injected (n=4). Following a 1-week acclimatization period, the treatment group had 0.4mg/mL STE (approximately 95mg/kg/day) supplemented in their drinking water ad libitum or 50mg/kg LPE in PBS injected intraperitoneally 3x per week. After a 4-week time period, mice were sacrificed using a CO_2 chamber and cervical dislocation, and organ tissues (liver, heart, kidney) were harvested for analysis. Organs were sent to the University of Guelph Animal Health Laboratory for histopathological analysis. Note that groups C1 (control), T5 (LPE), and T6 (STE) in the attached pathology report are relevant for this project.

Conclusion

In this study, we analyzed the overall implications of Long Pepper extract and Synthite Tea extract alone and in combination with standard chemotherapeutics cisplatin and TMZ on neuroblastoma and glioblastoma. We observed dose-dependent cell death following LPE or STE treatment alone, with STE enhancing the effects of cisplatin and TMZ *in-vitro* and LPE having no negative influence. LPE functions through multiple mechanisms to induce apoptosis including the overproduction of ROS and associated mitochondrial destabilization. Alternatively, STE functions primarily through the diminishment of the MMP. Though we did not analyze the ability of these extracts to cross the Blood Brain Barrier (BBB), previous research has shown piperlongumine and its analogues can cross the BBB [68,69], as can piperine and its closely related compounds [70,71]. Similarly, both green tea and its bioactive polyphenols have been shown to cross the BBB in prior works [72,73]. Importantly, our extracts display high tolerability to normal healthy cells with limited to no adverse effects *in-vivo*. Notably, in highly resistant GBM, CSCs were more sensitive to treatment with both STE and LPE compared to TMZ, demonstrating potential to reduce tumor relapse rate and treatment resistance. Therefore, STE and LPE should be investigated through additional *in-vivo* studies and clinical trials as potential therapeutics for both neuroblastoma and glioblastoma. Alongside standard chemotherapies, these extracts could drastically improve both quality of life and patient prognosis,

allowing for reduced dosages of chemotherapy and limited adverse effects [74].

Materials and Methods

2D cell culture

Human glioblastoma cells (U-87 Mg) derived from malignant glioma (ATCC, Cat. No. HTB-14, Manassas, VA, USA), human neuroblastoma cells (SH-SY5Y) derived from a metastatic bone tumour (ATCC, Cat. No. CRL-2266, Manassas, VA, USA), and normal human colon epithelial cells (NCM-460) (ATCC, Cat. No. CRL-1831, Manassas, VA, USA) were used throughout this study. U-87 Mg, SH-SY5Y, and NCM-460 cells were cultured in Eagle's Minimum Essential Medium with Earle's salts and nonessential amino acids, Dulbecco's Modified Eagle's Medium F-12 HAM, and Dulbecco's Modified Eagle Medium (Sigma-Aldrich, Mississauga, ON, Canada) respectively, all supplemented with 10% fetal bovine serum (Thermo Scientific, Waltham, MA, USA) and 10mg/mL gentamicin (Gibco BRL, VWR, Mississauga, ON, Canada). All cells were maintained at 37 °C and 5% CO_2.

Chemicals and cell treatment

a) Long Pepper Extract provided by Synthite Industries, India was dissolved in Dimethylsulfoxide (DMSO), and stock solutions were stored at -20 °C for no more than 2 weeks until use. Cells were treated at concentrations ranging from 0.025mg/mL to 0.5mg/mL.

b) Synthite Green Tea Extract provided by Synthite Industries, India was dissolved in double distilled milliQ water and stored at -20 °C until use. Cells were treated at concentrations ranging from 0.0125mg/mL to 0.2mg/mL.

c) Cisplatin (Sigma-Aldrich Canada, Cat. No. PHR1624) was dissolved in a 0.9% NaCl solution and stored at -20 °C until use. Cells were treated at doses ranging from 0.5μM to 5μM.

d) Temozolomide (Ontario Chemicals Inc., Cat. No. T1062) was dissolved in DMSO and stored at -20 °C until use. Cells were treated at concentrations ranging from 4μg/mL to 75μg/mL.

e) N-Acetyl-L-Cysteine (Sigma-Aldrich Canada, Cat. No. A7250) was dissolved in double distilled milliQ water and stored at -20 °C until use. Cells were treated at doses of 3mM for all experiments.

Analysis of cell death through annexin v and propidium iodide staining

Annexin V (AV) and Propidium Iodide (PI) fluorescent stains were used to visualize and quantify apoptotic and necrotic cells. Cells were seeded on 6-well plates 24 hours prior to treatment. Following treatment for 24 or 48hours, cells were collected, washed with Phosphate-Buffered Saline (PBS), and resuspended in Annexin V Binding Buffer (10mM HEPES, 140mM NaCl, 2.5mM CaCl2, pH 7.4). Annexin V Alexa Fluor™ 488 dye (1:20; Life Technologies Inc., Cat. No. A13201, Burlington, ON, Canada) and 0.01 mg/mL PI dye (Life Technologies Inc., Cat. No. P3566, Burlington, ON, Canada) were added and cells were incubated for 15 minutes at 37 °C and 5% CO_2 in the absence of light. Cells were quantified through flow cytometry using a Countess TM 3 Automated Cell Counter or imaged using epifluorescence microscopy following the addition of 10μM Hoechst nuclear stain with a Leica DMI6000 B inverted microscope and quantified with ImageJ software.

3D spheroid cell culture

Matrigel 3D tissue culturing was used to establish physiologically relevant cell environments with strong cell proliferation. Three-dimensional spheroid cultures were generated on tissue culture plates coated with Matrigel, a solubilized basement membrane matrix extract (Corning Life Sciences, Bedford, MA, USA). Matrigel quickly polymerizes into an irreversible gel form at 6-8 °C, therefore Matrigel aliquots were stored at -20 °C and thawed overnight on ice at 4 °C prior to use. For optimal spheroid formation conditions, 96-well tissue culture plates and pipette tips were chilled at -20 °C overnight. Chilled 96-well plates were coated with 35μL of liquid Matrigel using chilled pipette tips and incubated 37 °C for 30 minutes to achieve a solidified matrix. 4000-6000 U-87 Mg cells were seeded on coated 96-well plates and grown in media supplemented with 2% (v/v) Matrigel for 96 h with 5% CO_2 at 37 °C. Following incubation, media was replaced and replenished with 2% (v/v) Matrigel and spheroids were treated with LPE or STE for 96h. Spheroids were imaged using brightfield microscopy at 200x magnification using LAS AF6000 software and a Leica DMI600 florescent microscope.

Immunofluorescent staining for CD44 expression in GBM

To qualitatively identify and analyze glial cancer stem cells, U-87 Mg cells were seeded on 8-chamber slides, treated, and examined with immunofluorescent staining. Cells were treated for 48hours with TMZ, LPE, and STE prior to staining. Cells were fixed with 4% formaldehyde for 15minutes at room temperature and permeabilized with 0.15% Triton X-100 for 2minutes. Next, cells were blocked with 5% bovine serum albumin in PBS for 1hour, washed with Tris-buffered saline, 0.1% Tween 20 detergent (TBST), and incubated for 1 hour at room temperature with a CD44 primary antibody (mouse IgG, 1:100, No. ab6124) (Abcam Inc.). Cells were subsequently washed 5 times with TBST and incubated for 1 hour at room temperature with donkey anti-mouse Alexa FluorTM 488 (1:1000, Thermo Scientific Canada, Cat. No. A21202). Next, we performed five TBST washes and incubated cells with 10μM Hoechst 3342 (Molecular Probes, Cat. No. H3570, Eugene, OR, USA) for 2minutes. Finally, cells were washed with PBS and imaged using epifluorescence microscopy with a Leica DMI6000 B inverted microscope. Cells from at least 6 random fields were examined for each treatment.

Analysis of cellular motility using a wound-healing migration assay

In accordance with a previously published protocol,[23] cells were seeded on 6-well tissue culture plates and washed with PBS to remove any loosely bound cells. A sterile P200μL pipet tip was used to mechanically remove cells on a vertical line through each well. Pre-treatment with thymidine for 18 hours halted cell proliferation

and was followed by the addition of LPE or STE. Migration of the cells was monitored with light microscopy at 0-, 24-, and 48-hour timepoints. The wound closure by the migrating cells was measured at each time point.

WST-1 assay for cell viability

The WST-1 based colorimetric assay was conducted according to the manufacturer's protocol (Roche Applied Sciences, Indianapolis, IN, USA) to quantify cell viability through its correlation with active metabolism. Cells were seeded on 96-well cell culture plates and treated for the indicated time periods. Cells were then incubated with WST-1 reagent for 3hours at 37 °C and 5% CO_2 in the absence of light. WST-1 is cleaved by metabolically active cells to formazan which was detected through absorbance readings at 450nm on a Wallac Victor3 1420 Multilabel Counter.

Tetramethylrhodamine, methyl ester (TMRM) staining to analyze mitochondrial health

Intact mitochondrial membrane potentials were determined with the cell permeant dye TMRM (Gibco BRL, VWR, Mississauga, ON, Canada) which accumulates in healthy mitochondria. Cells were seeded on 6-well tissue culture plates and treated for 24 or 48hours. 100nM TMRM was added, and cells were incubated for 45 minutes at 37 °C. Cells were then washed, resuspended in PBS, and subjected to flow cytometric analysis using a CountessTM 3 Automated Cell Counter. Alternatively, cells were resuspended in PBS and counterstained with 10μM Hoechst 3342 (Molecular Probes, Cat. No. H3570, Eugene, OR, USA) before undergoing epifluorescence microscopy with a Leica DMI6000 B inverted microscope (Leica Microsystems, Concord, ON, Canada). ImageJ software was used to quantify fluorescence.

Measurement of reactive oxygen species via 2,7-Dichlorofluorescein (DCF) live cell fluorescent staining. Reactive Oxygen Species (ROS) levels were determined through H2DCFDA (Life Technologies Inc., Cat. No. D-399, Burlington, ON, Canada) staining which is oxidized to the fluorescent molecule DCF following cleavage in the presence of ROS. Cells were seeded in 6-well plates 24hours prior to treatment. Cells were treated for 3 or 24 hours before the addition of 10 μM H2DCFDA for 30minutes. Cells were incubated in the absence of light at 37 °C and 5% CO_2. Cells were washed and resuspended in PBS prior to flow cytometry analysis on a CountessTM 3 Automated Cell Counter. Alternatively, 10μM Hoechst 3342 (Molecular Probes, Cat. No. H3570, Eugene, OR, USA) was added and cells were imaged through epifluorescence microscopy with a Leica DMI6000 B inverted microscope. ImageJ software was utilized for fluorescent quantification.

Statistical analysis

All statistical analysis was performed using GraphPad Prism 6 statistical software where statistically significant values of $p<0.05$ are indicated by *, $p<0.01$ are indicated by **, $p<0.001$ are indicated by ***, and $p<0.0001$ are indicated by ****. Experiments involving the measurement of a single variable including analysis of ROS, Mitochondrial Membrane Potential (MMP), or GSCs were analyzed using 1-way analysis of variance (ANOVA) with Dunnett's test with each sample's mean compared to the negative DMSO control unless otherwise stated. In experiments involving multiple variables such as the quantification of living and dead cells, 2-way ANOVA with Dunnett's test was utilized and sample means were compared to the negative DMSO control unless otherwise specified. For the wound healing assay, simple linear regression was used to assess whether the slopes were significantly non-zero.

Acknowledgement

We gratefully acknowledge MITACS in collaboration with Synthite India Ltd for funding this work. The authors would like to acknowledge Anumita Jain, Ben Scaria, Eesha Bhagirath, Karthik Baskaran, and Mohammad El Hindawi for their technical help.

Author Contributions

Conceptualization, D.W., K.K., and S.P.; methodology, D.W., K.K., and S.P.; validation, D.W.; formal analysis, D.W.; investigation, D.W., K.K., M.O., C.V., I.A., and V.I.; resources, S.P.; writing - original draft preparation, D.W.; writing - review and editing, D.W., K.K., and S.P.; visualization, D.W. and K.K.; supervision, S.P.; project administration, D.W. and S.P.; funding acquisition, D.W. and S.P. All authors have read and agreed to the published version of the manuscript.

Data Availability

The data presented in this study are available.

Competing Interests

No potential competing interest was reported by the authors.

References

1. Alexander F (2000) Neuroblastoma. Urol Clin North Am 27: 383-392.
2. Matthay KK, Maris JM, Schleiermacher G, Nakagawara A, Mackall CL, et al. (2016) Neuroblastoma. Nat Rev Dis Primers 2: 16078.
3. Matthay KK, Villablanca JG, Seeger RC, Stram DO, Harris RE, et al. (1999) Treatment of high-risk neuroblastoma with intensive chemotherapy, radiotherapy, autologous bone marrow transplantation, and 13-cis-retinoic acid. N Engl J Med 341(16): 1165-1173.
4. Grochans S, Cybulska AM, Simińska D, Korbecki J, Kojder K, et al. (2022) Epidemiology of glioblastoma multiforme-literature review. Cancers (Basel) 14(10): 2412.
5. Ostrom QT, Gittleman H, Farah P, Ondracek A, Chen Y, et al. (2013) CBTRUS statistical report: Primary brain and central nervous system tumors diagnosed in the United States in 2006-2010. Neuro Oncol 15 Suppl 2(Suppl 2): ii1-ii56.
6. Yabroff KR, Harlan L, Zeruto C, Abrams J, Mann B (2012) Patterns of care and survival for patients with glioblastoma multiforme diagnosed during 2006. Neuro Oncol 14(3): 351-359.
7. Yamasaki F, Kurisu K, Satoh K, Arita K, Sugiyama K, et al. (2005) Apparent diffusion coefficient of human brain tumors at MR imaging. Radiology 235(3): 985-991.
8. Carlsson SK, Brothers SP, Wahlestedt C (2014) Emerging treatment strategies for glioblastoma multiforme. EMBO Mol Med 6(11): 1359-1370.
9. Mukherjee B, McEllin B, Camacho CV, Tomimatsu N, Sirasanagandala S, et al. (2009) EGFRvIII and DNA double-strand break repair: A molecular mechanism for radioresistance in glioblastoma. Cancer Res 69(10): 4252-4259.

10. Stupp R, Mason WP, Bent MJVD, Weller M, Fisher B, et al. (2005) Radiotherapy plus concomitant and adjuvant temozolomide for glioblastoma. N Engl J Med 352(10): 987-996.

11. Villalva C, Cortes U, Wager M, Tourani JM, Rivet P, et al. (2012) O6-Methylguanine-Methyltransferase (MGMT) promoter methylation status in glioma stem-like cells is correlated to temozolomide sensitivity under differentiation-promoting conditions. Int J Mol Sci 13(6): 6983-6994.

12. Cheng L, Wu Q, Guryanova OA, Huang Z, Huang Q, et al. (2011) Elevated invasive potential of glioblastoma stem cells. Biochem Biophys Res Commun 406(4): 643-648.

13. Alves ALV, Gomes INF, Carloni AC, Rosa MN, Silva LSD, et al. (2021) Role of glioblastoma stem cells in cancer therapeutic resistance: A perspective on antineoplastic agents from natural sources and chemical derivatives. Stem Cell Research & Therapy 12(1): 206.

14. Lathia JD, Mack SC, Hubert EEM, Valentim CLL, Rich JN (2015) Cancer stem cells in glioblastoma. Genes Dev 29: 1203-1217.

15. Singh SK, Hawkins C, Clarke ID, Squire JA, Bayani J, et al. (2004) Identification of human brain tumour initiating cells. Nature 432(7015): 396-401.

16. Inoue A, Ohnishi T, Nishikawa M, Ohtsuka Y, Kusakabe K, et al. (2023) A narrative review on CD44's role in glioblastoma invasion, proliferation, and tumor recurrence. Cancers (Basel) 15(19): 4898.

17. Bernonville TD, Clastre M, Besseau S, Oudin A, Burlat V, et al. (2015) Phytochemical genomics of the Madagascar periwinkle: Unravelling the last twists of the alkaloid engine. Phytochemistry 113: 9-23.

18. Wani MC, Taylor HL, Wall ME, Coggon P, McPhail AT (1971) Plant antitumor agents. VI. Isolation and structure of taxol, a novel antileukemic and antitumor agent from *Taxus brevifoli*. J Am Chem Soc 93(9): 2325-2327.

19. Ovadje P, Roma A, Steckle M, Nicoletti L, Arnason JT, et al. (2015) Advances in the research and development of natural health products as main stream cancer therapeutics. Evid Based Complement Alternat Med 2015: 751348.

20. Ovadje P, Ma D, Tremblay P, Roma A, Steckle M, et al. (2014) Evaluation of the efficacy & biochemical mechanism of cell death induction by piper longum extract selectively in *in-vitro* and *in-vivo* models of human cancer cells. PLoS One 9(11): e113250.

21. Philion C, Ma D, Ruvinov I, Mansour F, Pignanelli C, et al. (2017) *Cymbopogon citratus* and *Camellia sinensis* extracts selectively induce apoptosis in cancer cells and reduce growth of lymphoma xenografts *in vivo*. Oncotarget 8(67): 110756-110773.

22. Nguyen C, Mehaidli A, Baskaran K, Grewal S, Pupulin A, et al. (2019) Dandelion root and lemongrass extracts induce apoptosis, enhance chemotherapeutic efficacy, and reduce tumour xenograft growth *in vivo* in prostate cancer. Evid Based Complement Alternat Med 2019: 2951428.

23. Ovadje P, Ammar S, Guerrero JA, Arnason JT, Pandey S (2016) Dandelion root extract affects colorectal cancer proliferation and survival through the activation of multiple death signalling pathways. Oncotarget 7(45): 73080-73100.

24. Ovadje P, Hamm C, Pandey S (2012) Efficient induction of extrinsic cell death by dandelion root extract in human Chronic Myelomonocytic Leukemia (CMML) cells. PLoS One 7(2): e30604.

25. Nguyen C, Baskaran K, Pupulin A, Ruvinov I, Zaitoon O, et al. (2019) *Hibiscus* flower extract selectively induces apoptosis in breast cancer cells and positively interacts with common chemotherapeutics. BMC Complement Altern Med 19(1): 98.

26. Raad C, Raad A, Pandey S (2024) Green tea leaves and rosemary extracts selectively induce cell death in triple-negative breast cancer cells and cancer stem cells and enhance the efficacy of common chemotherapeutics. Evidence-Based Complementary and Alternative Medicine 2024: 9458716.

27. Adams DJ, Dai M, Pellegrino G, Wagner BK, Stern AM, et al. (2012) Synthesis, cellular evaluation, and mechanism of action of piperlongumine analogs. Proc Natl Acad Sci U S A 109(38): 15115-15120.

28. Yaffe PB, Doucette CD, Walsh M, Hoskin DW (2013) Piperine impairs cell cycle progression and causes reactive oxygen species-dependent apoptosis in rectal cancer cells. Exp Mol Pathol 94(1): 109-114.

29. Ravindranath MH, Saravanan TS, Monteclaro CC, Presser N, Ye X, et al. (2006) Epicatechins purified from green tea (*Camellia sinensis*) differentially suppress growth of gender-dependent human cancer cell lines. Evid Based Complement Alternat Med 3(2): 237-247.

30. Manian R, Anusuya N, Siddhuraju P, Manian S (2008) The antioxidant activity and free radical scavenging potential of two different solvent extracts of *Camellia sinensis* (L.) O. Kuntz, *Ficus bengalensis L.* and *Ficus racemosa L*. Food Chemistry 107: 1000-1007.

31. Toden S, Tran HM, Camargo OAT, Okugawa Y, Goel A (2016) Epigallocatechin-3-gallate targets cancer stem-like cells and enhances 5-fluorouracil chemosensitivity in colorectal cancer. Oncotarget 7(13): 16158-16171.

32. Miyata Y, Shida Y, Hakariya T, Sakai H (2019) Anti-cancer effects of green tea polyphenols against prostate cancer. Molecules 24(1): 193.

33. Samavat H, Ursin G, Emory TH, Lee E, Wang R, et al. (2017) A randomized controlled trial of green tea extract supplementation and mammographic density in postmenopausal women at increased risk of breast cancer. Cancer Prev Res (Phila) 10(12): 710-718.

34. Abdelhamed S, Yokoyama S, Refaat A, Ogura K, Yagita H, et al. (2014) Piperine enhances the efficacy of TRAIL-based therapy for triple-negative breast cancer cells. Anticancer Res 34(4): 1893-1899.

35. Greenshields AL, Doucette CD, Sutton KM, Madera L, Annan H, et al. (2015) Piperine inhibits the growth and motility of triple-negative breast cancer cells. Cancer Lett 357(1): 129-140.

36. Aumeeruddy MZ, Mahomoodally MF (2019) Combating breast cancer using combination therapy with 3 phytochemicals: Piperine, sulforaphane, and thymoquinone. Cancer 125(10): 1600-1611.

37. Samykutty A, Shetty AV, Dakshinamoorthy G, Bartik MM, Johnson GL, et al. (2013) Piperine, a bioactive component of pepper spice exerts therapeutic effects on androgen dependent and androgen independent prostate cancer cells. PLoS One 8: e65889.

38. Makhov P, Golovine K, Canter D, Kutikov A, Simhan J, et al. (2012) Co-administration of piperine and docetaxel results in improved anti-tumor efficacy via inhibition of CYP3A4 activity. Prostate 72(6): 661-667.

39. Ouyang D, Ouyang DY, Zeng LH, Pan H, Xu LH, et al. (2013) Piperine inhibits the proliferation of human prostate cancer cells via induction of cell cycle arrest and autophagy. Food Chem Toxicol 60: 424-430.

40. Yaffe PB, Coombs MRP, Doucette CD, Walsh M, Hoskin DW (2015) Piperine, an alkaloid from black pepper, inhibits growth of human colon cancer cells via G1 arrest and apoptosis triggered by endoplasmic reticulum stress. Mol Carcinog 54(10): 1070-1085.

41. Ma D, Gilbert T, Pignanelli C, Tarade D, Noel M, et al. (2018) Exploiting mitochondrial and oxidative vulnerabilities with a synthetic analog of pancratistatin in combination with piperlongumine for cancer therapy. FASEB Journal 32(1): 417-430.

42. Lv D, Hu Z, Lu L, Lu H, Xu X (2017) Three-dimensional cell culture: A powerful tool in tumor research and drug discovery. Oncol Lett 14(6): 6999-7010.

43. Edmondson R, Broglie JJ, Adcock AF, Yang L (2014) Three-dimensional cell culture systems and their applications in drug discovery and cell-based biosensors. Assay Drug Dev Technol 12(4): 207-218.

44. Marzagalli M, Fontana F, Raimondi M, Limonta P (2021) Cancer stem cells-key players in tumor relapse. Cancers (Basel) 13(3): 376.

45. Chan KS (2016) Molecular pathways: Targeting cancer stem cells awakened by chemotherapy to abrogate tumor repopulation. Clin Cancer Res 22(4): 802-806.

46. Cunha MLVD, Maldaun MVC (2019) Metastasis from glioblastoma multiforme: A meta-analysis. Rev Assoc Med Bras 65(3): 424-433.

47. Seo YJ, Cho WH, Kang DW, Cha SH (2012) Extraneural metastasis of glioblastoma multiforme presenting as an unusual neck mass. J Korean Neurosurg Soc 51(3): 147-150.

48. Berthold F, Spix C, Kaatsch P, Lampert F (2017) Incidence, survival, and treatment of localized and metastatic neuroblastoma in Germany 1979-2015. Paediatr Drugs 19(6): 577-593.

49. Dürr D, Stieger B, Ublick GAK, Rentsch KM, Steinert HC, et al. (2000) St John's wort induces intestinal P-glycoprotein/MDR1 and intestinal and hepatic CYP3A4. Clinical Pharmacology & Therapeutics 68(6): 598-604.

50. Comelli MC, Mengs U, Schneider C, Prosdocimi M (2007) Toward the definition of the mechanism of action of silymarin: activities related to cellular protection from toxic damage induced by chemotherapy. Integr Cancer Ther 6(2): 120-129.

51. Bezerra DP, Pessoa C, Moraes MOD, Neto NS, Silveira ER, et al. (2013) Overview of the therapeutic potential of piplartine (piperlongumine). European Journal of Pharmaceutical Sciences 48(3): 453-463.

52. Gorrini C, Harris IS, Mak TW (2013) Modulation of oxidative stress as an anticancer strategy. Nat Rev Drug Discov 12(12): 931-947.

53. Nakagawara A, Li Y, Izumi H, Muramori K, Inada H, et al. (2018) Neuroblastoma. Japanese Journal of Clinical Oncology 48(3): 214-241.

54. Warburg O (1956) On respiratory impairment in cancer cells. Science 124(3215): 269-270.

55. Wang X, Wang W, Li L, Perry G, Lee HG, et al. (2014) Oxidative stress and mitochondrial dysfunction in Alzheimer's disease. Biochim Biophys Acta 1842(8): 1240-1247.

56. Shimizu M, Adachi S, Masuda M, Kozawa O, Moriwaki H (2011) Cancer chemoprevention with green tea catechins by targeting receptor tyrosine kinases. Molecular Nutrition & Food Research 55(6): 832-843.

57. Singh BN, Shankar S, Srivastava RK (2011) Green tea catechin, epigallocatechin-3-gallate (EGCG): Mechanisms, perspectives and clinical applications. Biochem Pharmacol 82(12): 1807-1821.

58. Lee JJ, Lee JH, Ko YG, Hong SI, Lee JS (2010) Prevention of premature senescence requires JNK regulation of Bcl-2 and reactive oxygen species. Oncogene 29(4): 561-575.

59. Lei K, Nimnual A, Zong WX, Kennedy NJ, Flavell RA, et al. (2002) The bax subfamily of Bcl2-related proteins is essential for apoptotic signal transduction by c-Jun NH2-terminal kinase. Mol Cell Biol 22(13): 4929-4942.

60. Lee SY (2016) Temozolomide resistance in glioblastoma multiforme. Genes & Diseases 3(3): 198-210.

61. Conklin KA (2004) Chemotherapy-associated oxidative stress: Impact on chemotherapeutic effectiveness. Integr Cancer Ther 3(4): 294-300.

62. Bedrood Z, Rameshrad M, Hosseinzadeh H (2018) Toxicological effects of *Camellia sinensis* (green tea): A review. Phytotherapy Research 32(7): 1163-1180.

63. Lee SB, Choi EH, Jeong KH, Kim KS, Shim SM, et al. (2020) Effect of catechins and high-temperature-processed green tea extract on scavenging reactive oxygen species and preventing Aβ1-42 fibrils' formation in brain microvascular endothelium. Nutritional Neuroscience 23(5): 363-373.

64. Bezerra DP, Castro FO, Alves APNN, Pessoa C, Moraes MO, et al. (2006) *In vivo* growth-inhibition of Sarcoma 180 by piplartine and piperine, two alkaloid amides from Piper. Braz J Med Biol Res 39(6): 801-807.

65. Bezerra DP, Castro FOD, Alves APNN, Pessoa C, Moraes MOD, et al. (2008) *In vitro* and *in vivo* antitumor effect of 5-FU combined with piplartine and piperine. Journal of Applied Toxicology 28(2): 156-163.

66. Lin Y, Xu J, Liao H, Li L, Pan L (2014) Piperine induces apoptosis of lung cancer A549 cells via p53-dependent mitochondrial signaling pathway. Tumour Biol 35(4): 3305-3310.

67. Almeida GCD, Oliveira LFS, Predes D, Fokoue HH, Kuster RM, et al. (2020) Piperine suppresses the Wnt/β-catenin pathway and has anti-cancer effects on colorectal cancer cells. Sci Rep 10(1): 11681.

68. Martins IJ (2018) Sirtuin 1, a diagnostic protein marker and its relevance to chronic disease and therapeutic drug interventions. EC Pharmacology and Toxicology 6.4(2018): 209-215.

69. Liu H, Luo R, Chen X, Liu J, Bi Y, et al. (2013) Tissue distribution profiles of three antiparkinsonian alkaloids from *Piper longum* L. in rats determined by liquid chromatography-tandem mass spectrometry. J Chromatogr B Analyt Technol Biomed Life Sci 928: 78-82.

70. Ji L, Qu L, Wang C, Peng W, Li S, et al. (2021) Identification and optimization of piperlongumine analogues as potential antioxidant and anti-inflammatory agents via activation of Nrf2. European Journal of Medicinal Chemistry 210: 112965.

71. Eigenmann DE, Dürig C, Jähne EA, Smieško M, Culot M, et al. (2016) *In vitro* blood-brain barrier permeability predictions for GABAA receptor modulating piperine analogs. European Journal of Pharmaceutics and Biopharmaceutics 103: 118-126.

72. Baghdadi OBA, Prater NI, Schyf CJVD, Geldenhuys WJ (2012) Inhibition of monoamine oxidase by derivatives of piperine, an alkaloid from the pepper plant *Piper nigrum*, for possible use in Parkinson's disease. Bioorganic & Medicinal Chemistry Letters 22(23): 7183-7188.

73. Ye Q, Ye L, Xu X, Huang B, Zhang X, et al. (2012) Epigallocatechin-3-gallate suppresses 1-methyl-4-phenyl-pyridine-induced oxidative stress in PC12 cells via the SIRT1/PGC-1α signaling pathway. BMC Complement Altern Med 12: 82.

74. Weinreb O, Mandel S, Amit T, Youdim MBH (2004) Neurological mechanisms of green tea polyphenols in Alzheimer's and Parkinson's diseases. The Journal of Nutritional Biochemistry 15(9): 506-516.